Large-Scale Simulation of Flow and Transport in Reconstructed Porous Media

Siarhei Khirevich,[1] Alexandra Höltzel,[1] Dzmitry Hlushkou,[1] Andreas Seidel-Morgenstern,[2] and Ulrich Tallarek[1]

[1]Department of Chemistry, Philipps-Universität Marburg, Hans-Meerwein-Strasse, 35032 Marburg, Germany
E-mail addresses: khirevic@staff.uni-marburg.de, tallarek@staff.uni-marburg.de
[2]Max Planck Institute for Dynamics of Complex Technical Systems, Sandtorstrasse 1, 39106 Magdeburg, Germany

Introduction

The micro total analysis systems (μTAS) are of great interest for many applications in the life sciences and medicinal diagnostics. μTAS, also called “lab-on-a-chip”, ideally integrate a complete analytical process (including sample preparation, injection, separation, and detection) in a microfluidic chip format and enable an analysis of a huge number of complex samples available only in minute quantities. Microchannels, the crucial parts of μTAS, play a number of roles in microchips, such as transport of liquids between microchip parts, mixing reagents, performance of reaction. In this work, we analyze flow and transport in reconstructed microchannels by employing quantitative numerical simulation methods and an efficient use of supercomputer resources.

Reconstruction of the microchannel and packing generation

This work[1] is based on a prototype HPLC/UV-microchip that integrates sample injection, chromatographic separation, and UV detection (Figure 1). The reconstruction step in our work includes the following:

- **reconstruction of the microchannel cross-section,**
- **experimentally determined particle size distribution (5 μm Zorbax SB-C18 material), and**
- **average interparticle porosity (packing density, ε).**

To validate our approach, we simulated flow and dispersion in the empty channel of the reconstructed cross-section. According to the Figure 2a, simulation results for the unpacked reconstructed microchannel agree very well with experimental data. Hereafter, packings containing about 330 000 particles were generated using collective-rearrangement algorithm (Jodrey-Tory). Figures 2b and 2c show the front view, projections of the particle centers and porosity distributions of the generated packings.

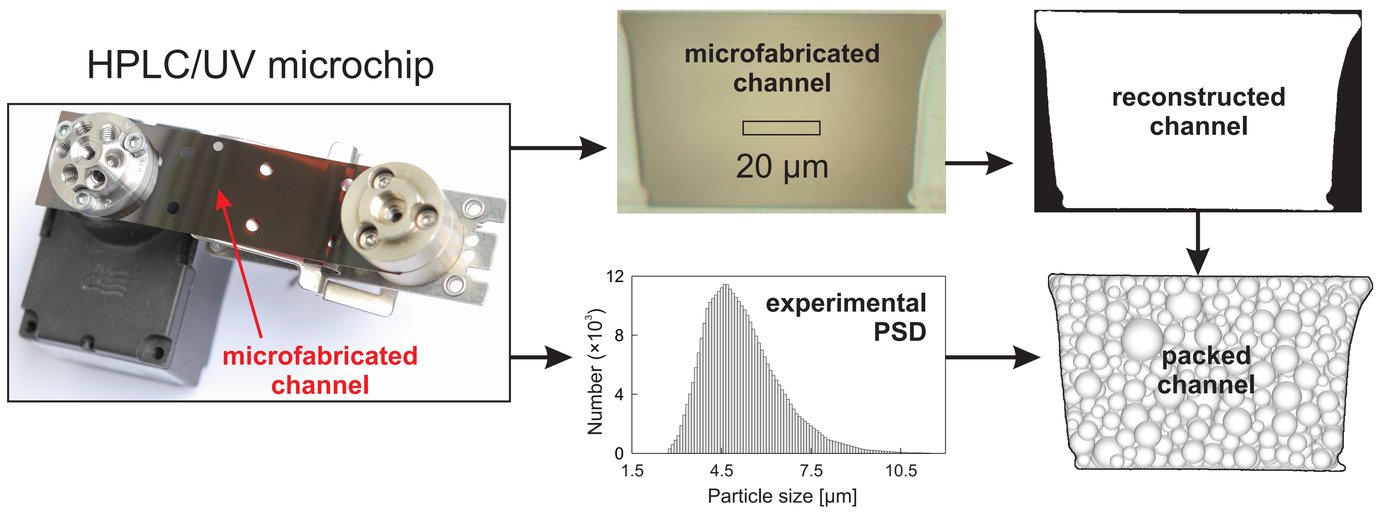

Figure 1. The workflow of the reconstruction step in our work. Left: a prototype HPLC/UV-microchip; the microchip is placed between the stator and rotor of a Rheodyne valve, and the end containing the UV-detection cell is fixed by a holder for connection to a diode array UV detector. Top center: a photograph of the microchannel cross-section. Top right: reconstructed channel. Bottom center: experimentally determined particle-size distribution of the packing material. Bottom right: generated packing.

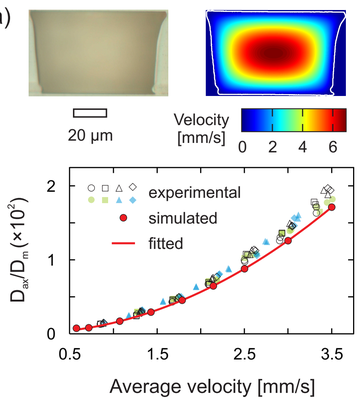

Figure 2. a) Lateral velocity distribution (averaged over the channel length) at an average velocity of 3 mm/s and axial hydrodynamic dispersion in the unpacked reconstructed microchannel. Simulated data are fitted to equation[2] $D_{ax}/D_m = 1 + (F/210)\,Pe^2$, where $Pe = u_{av}d_p/D_m$ is the Péclet number and $F = 2.62$. Experimental data were collected with several prototype HPLC/UV-microchips (each symbol refers to one microchip). **b)** Reconstructed microchip packings of low (ε = 0.42) and high (ε = 0.48) bed porosity. Left: front view onto the packing cross-section, middle: projection of particle centers onto the front plane, and right: lateral porosity distribution averaged over the whole packing length. **c)** Porosity distribution along both diagonals of the channel cross-section (averaged over the whole packing length).

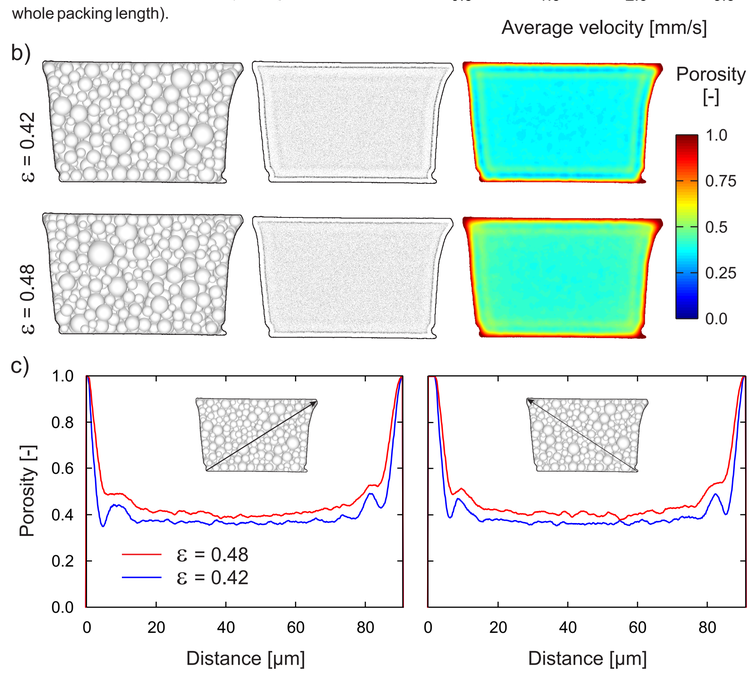

Simulation details

The simulations were performed in three consecutive steps: i) generation of random packings of solid, impermeable spherical particles using the modified Jodrey-Tory (JT) procedure, ii) simulation of flow within the interparticle void space involving the Lattice-Boltzmann method, and iii) simulation of convective-diffusive mass-transport using the random walk particle tracking method.

Figure 3. Average fluid velocity within the packing vs. lattice resolution. Dashed line shows the average velocity calculated with Kozeny–Carman equation. Red circle indicates the average lattice resolution employed in the simulations.

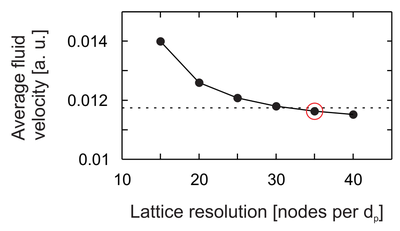

Figure 4. One-dimensional (”slice”) decomposition of (a,b) the grid containing porosity and fluid velocity fields and (b) tracers ensemble according to the longitudinal tracer coordinate.

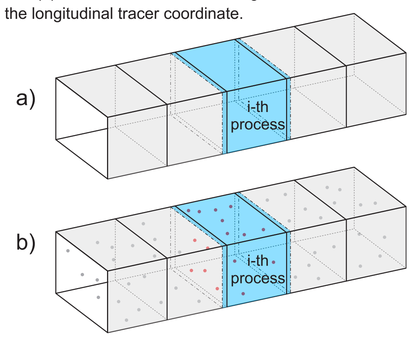

Figure 5. Performance scaling (gain in calculation time as a function of the number of processor cores used) of the algorithms employed for the calculation of 3D velocity fields (LBM, lattice-Boltzmann method) and axial hydrodynamic dispersion coefficients (RWPT, random-walk particle-tracking) for small and medium-sized problems. The achieved performance scaling which is nearly linear for both algorithms and problem sizes reflects the efficient use of supercomputer power.

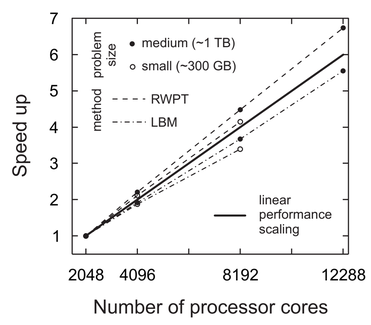

i) The JT-approach can be classified as a collective rearrangement algorithm. In each iteration step, the centers of two particles with the minimal distance from each other move apart and then the minimal pairwise distance between all the particle centers in the packing is recalculated. JT-procedure was originally developed to generate monodisperse packings with periodic boundaries along all spatial dimensions. Our modification of the JT-approach enables the generation of packings of non-uniform spheres packed in the containers of an arbitrary cross-section. Program algorithm generating packings was written in C language, is sequential (i.e., program was developed to be run on one processor), and has complexity of O(n). The algorithm allows us to generate packings of the average porosity of 40% and containing several millions of spheres.

After the packing is generated, it was discretized with the average spatial resolution of ~35 nodes per $d_p(N_{max})$. This resolution is fine enough for the accurate simulation of fluid flow in the random close sphere packings (Figure 3).

ii) To simulate the laminar flow of incompressible fluid within the interparticle void space, we involve the Lattice-Boltzmann method (LBM). LBM is a relatively new numerical approach and is an alternative to the traditional Eulerian methods (like finite difference or finite elements). Such advantages of the LBM as the local node update rule and easy handling of complex boundary conditions make the method an ideal candidate for the large-scale simulation of fluid flow in the random close sphere packings.

We implemented the parallel version of the LBM (i.e., wrote a program to be run on many processors) using C language and MPI communication library. During the running process, the program code creates the grid which contains porosity and velocity fields, divides the whole grid into smaller slices (Figure 4) and distributes these slices over allocated processors. Hereafter, each processor handles its own slice and communicates with other processors. One of the way to estimate the effectiveness of the parallel algorithm realization is to measure the performance scaling (that is the relative increase of the calculation speed with the increase of the number of processors allocated). “Strong” performance scaling, showed on the Figure 5, is the performance scaling by the fixed problem size while the processor number is varied (in our work, the problem size is the amount of the grid nodes to be processed). Achieved close to the linear performance scaling (Figure 5, curves for the LBM), indicates the good parallel effectiveness of the program code. One LBM simulation required 3000 iterations, 3TB memory space, and took about 1.5 h on the 8192 processor cores of an IBM BlueGene/P system.

iii) Advective-diffusive mass transport was simulated with the Random Walk Particle Tracking method (RWPT). As the LBM, the RWPT is an alternative approach too. The concept of RWPT is to displace large amount of tracer particles in the volume of interest and to track the spatial statistical moments (i.e., mean displacement, variance of displacement, etc.) of the tracer ensemble. Due to the independent update rule of each tracer particle coordinate, RWPT is well suited for parallel processing. Results for the strong performance scaling are presented on the Figure 5 and similar to those of the LBM program realization. In each simulation we used tracer ensemble of two million tracer particles. One RWPT simulation required 2TB memory space, and took from 0.3 to 1.7 h on the 8192 processor cores of an IBM BlueGene/P system.

Flow and mass transport simulation results

- **Particle size distribution with non-zero variance damps porosity and fluid velocity oscillations near the channel wall (Figure 6).**
- **Irregularly shaped space in the channel corners is the location of advanced fluid flow (Figure 6).**
- **Higher average fluid velocity decreases equilibration time (Figure 7).**
- **Compared to monodisperse packings[3], in polydisperse packed beds the porosity influence on axial hydrodynamic dispersion is reduced (Figure 7b, left).**
- **At the low bed porosity packings (ε = 0.42) experimental dispersion coefficients are lower than simulated data (Figure 7b, right).**
- **According to SEM images, microchannel corners are packed more tightly than corners of generated packings (Figure 7c).**

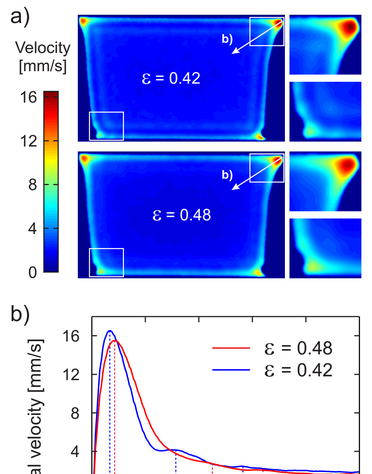

Figure 6. a) Lateral velocity distribution (averaged over the packing length) in reconstructed microchip packings of low (ε = 0.42) and high (ε = 0.48) bed porosity at a reduced linear velocity of $Pe = u_{av}d_p/D_m = 10$. The top right and bottom left corner regions are shown as enlargements. **b)** 1D velocity distribution in the top right channel corner for both packings taken along the arrow indicated in the images above. Dashed vertical lines denote maxima in the velocity distributions.

Figure 7. a) Left: axial hydrodynamic dispersion coefficient as a function of time; right: equilibration time (time after which asymptotic behavior in D_{ax}/D_m is observed). **b)** Left: normalized asymptotic axial hydrodynamic dispersion coefficients D_{ax}/D_m as a function of the Péclet number ($Pe = u_{av}d_p/D_m$) for the reconstructed microchip packings; right: comparison of axial hydrodynamic dispersion in the reconstructed microchip packings with experimental data from HPLC/UV-microchips (slurry-packed under the indicated conditions with 5 μm-sized Zorbax SB-C18 particles). **c)** Comparison of packing structure in the upper right channel corner of reconstructed and HPLC/UV-microchip packings (ε = 0.42). Reconstructed packings are represented by slices of ca. 10μm thickness, taken at random intervals along the packing length. SEM images of HPLC/UV-microchip packings were obtained from cutting orthogonally to the separation channel length. Note that the cutting process introduces additional surface roughness to the channel walls.

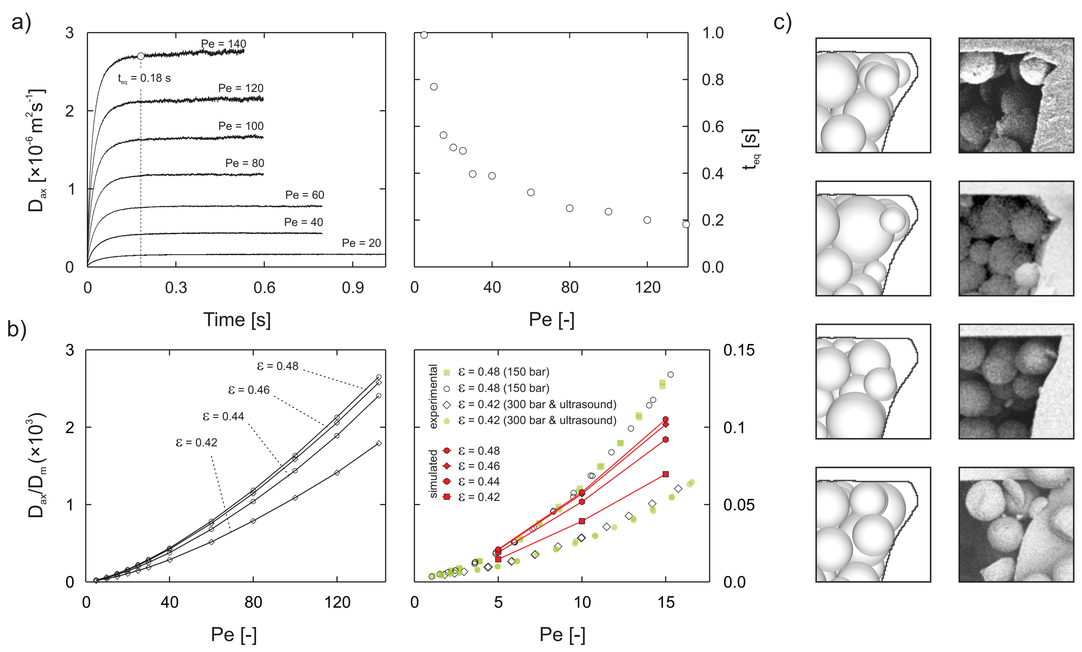

Acknowledgements

We thank RZG (Rechenzentrum Garching, Germany) and GWDG (Gesellschaft für wissenschaftliche Datenverarbeitung Göttingen, Germany) for providing computational resources and technical support.

References

(1) Khirevich, S.; Höltzel, A.; Ehlert, S.; Seidel-Morgenstern, A.; Tallarek, U. *Large-scale simulation of flow and transport in reconstructed HPLC-microchip packings.* Anal. Chem. **2009**, 81, 4937-4945.
(2) Dutta, D.; Ramachandran, A.; Leighton, D. T. *Effect of channel geometry on solute dispersion in pressure-driven microfluidic systems.* Microfluid. Nanofluid. **2006**, 2, 275-290.
(3) Khirevich, S.; Höltzel, A.; Hlushkou, D.; Tallarek, U. *Impact of conduit geometry and bed porosity on flow and dispersion in noncylindrical sphere packings.* Anal. Chem. **2007**, 79, 9340-9349.